

# Using cluster studies to approach the electronic structure of bulk water: Reassessing the vacuum level, conduction band edge, and band gap of water

James V. Coe, Alan D. Earhart, and Michael H. Cohen

*Department of Chemistry, The Ohio State University., 100 W. 18th Avenue, Columbus Ohio 43210-1173*

Gerald J. Hoffman<sup>a)</sup>

*Department of Chemistry, Pomona College, 645 N. College Avenue, Claremont, California 91711*

Harry W. Sarkas and Kit H. Bowen

*Department of Chemistry, Johns Hopkins University, N. Charles Street, Baltimore, Maryland 21218*

(Received 9 May 1997; accepted 21 July 1997)

Aqueous cluster studies have led to a reassessment of the electronic properties of bulk water, such as band gap, conduction band edge, and vacuum level. Using results from experimental hydrated electron cluster studies, the location of the conduction band edge relative to the vacuum level (often called the  $V_0$  value) in water has been determined to be  $-0.12 \text{ eV} \leq V_0 \leq 0.0 \text{ eV}$ , which is an order of magnitude smaller than most experimental values in the literature. With  $V_0 = -0.12 \text{ eV}$  and making use of the calculated solvation energy of OH in water, the band gap of water is determined to be 6.9 eV. Again, this is smaller than many literature estimates. In the course of this work, it is shown that due to water's ability to reorganize about charge (1) photoemission thresholds of water or anionic defects in water do not determine the vacuum level, and (2) there is almost no probability of accessing the bottom of the conduction band of water with a vertical/optical process from water's valence band. The results are presented in an energy diagram for bulk water which shows the utility of exploring the conduction band of water as a function of solvent polarization. © 1997 American Institute of Physics. [S0021-9606(97)02340-4]

## I. INTRODUCTION

The advent of large size range studies<sup>1-5</sup> dealing with the spectroscopy and energetics of aqueous clusters and cluster ions naturally leads to the examination of how these cluster properties evolve into their bulk counterparts. Such pursuits require a well-characterized picture of the bulk material. The electronic (amorphous semiconductor) properties of bulk water, such as the band gap and the location of the conduction band edge relative to the vacuum level, are not as well-characterized as one might think, primarily due to the ability of water to reorganize itself about charge. Any photoionization or photoemission process in water involves the loss of an electron from the initial state and, consequently, a difference in charge of the initial and final chemical entities. Thus the nascent products of vertical photoionization or photoemission processes inevitably find themselves with a configuration of solvent molecules far from equilibrium, even if there is no significant geometry change in the solute itself. The solvent reorganization energy (RE) in photoemission processes is the energy difference between the most probable product configuration (the one most like the initial state) and the final equilibrated arrangement of solvent molecules about the product. The magnitude of RE depends on the ion and solvent involved, but is large (1.5–5 eV) in water. As a result, there is little probability for directly observing a vertical transition between the valence

band edge and the conduction band edge of water, primarily because the structures associated with the arrangement of solvent molecules are so different in the equilibrated initial and final states of the photoemission process.

In the present work, an adiabatic value for the band gap of water has been determined by constructing thermochemical cycles that use the common  $\text{OH}^-$  defect state in water. Most of the required quantities are available except for a revised  $V_0$  value (the adiabatic energy of the conduction band's lower edge relative to the vacuum level) and  $\Delta E_{\text{sol}}(\text{OH})$  (the solvation energy of the anionic defect's corresponding radical). These two missing quantities are presently determined from cluster studies [ $V_0$  from experimental hydrated electron cluster studies and  $\Delta E_{\text{sol}}(\text{OH})$  theoretically]. Additionally, a standard picture of the electronic states of bulk water (a semiconductor picture) has been modified by explicit consideration of the energies associated with reorganization of solvating water molecules about charge. A bulk picture of water emerges which clearly distinguishes between adiabatic and the most-probable vertical processes, as well as the thresholds for vertical processes which can lie in between. Anionic cluster properties can be extrapolated to this framework with more clarity than was previously feasible.

### A. Basic relations in the photophysics of aqueous anionic defects

A pictorial definition of the energetic quantities associated with anionic defects in water is given in Fig. 1. In this diagram the most stable states (lowest energies) are placed at

<sup>a)</sup>Current address: Department of Chemistry, the College of New Jersey, P.O. Box 7718, Ewing, NJ 08628-0718.

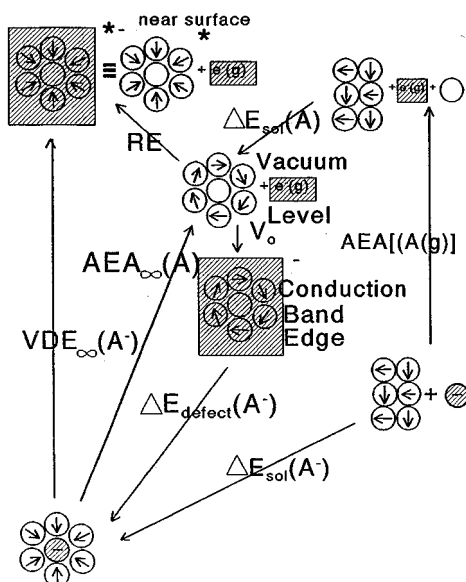


FIG. 1. Pictorial representation of the energetics of anionic defects in water distinguishing the vertical ( $VDE_{\infty}$ ) and adiabatic ( $AEA_{\infty}$ ) photoemission processes. The  $VDE_{\infty}$  process corresponds to the most probable transition energy, i.e., the geometry of the upper state is most like the geometry of the initial state. The  $AEA_{\infty}$  process corresponds to the minimum or adiabatic energy difference and is not readily accessible with a direct optical/vertical process. The up-down scale corresponds to energy with the most stable (lowest energy) states at the bottom. The arrows designate the direction of chemical equations defining the signs of the corresponding energetic quantities used throughout this paper. The excess charge in each state is represented by shading in a manner that depicts the delocalized electron states as large (in comparison to the size of solvent molecules) shaded boxes.

the bottom, and the least stable (highest energies) at the top. The most stable state (at the bottom) represents an anionic defect, which would lie energetically somewhere in the band gap of water. The solvating water molecules will optimally orient themselves about the charge in a manner which is very different from their alignment in the absence of charge. This is depicted in Fig. 1 by showing solvent dipoles directed toward the charge. The multidirectional, hydrogen-bonding capacity of water makes the actual structures involved more complicated, but the simple electrostatic picture captures the essential physics for the present purposes. If a photon of sufficient energy is absorbed by the anionic defect state, the excess electron can be excited into the conduction band, i.e., to a delocalized state with electron conducting character. The disorder associated with water's liquid nature (compared to a crystal) produces energetics similar to a large band gap, amorphous semiconductor.<sup>6-8</sup> The excited electron will not delocalize over the entire liquid, but rather over a limited region which is larger than an individual water molecule. This excited electron state is sometimes described as being "quasi-free" in which the electron is delocalized by comparison to the electrons bound to water molecules, but localized compared to the conducting electrons of metals. This process occurs vertically; i.e., the electron is excited on a timescale ( $< 10^{-15}$  s) much faster than the motion of the atomic nuclei involved. If near an electrode, the conducting or quasi-free electron could be detected as an electrical cur-

rent within the bulk material (photoconductivity). If near a surface, above the vacuum level, and above the photoemission threshold when reorganization energy is important, it can be emitted into vacuum (photoemission). The most probable transition energy for either the photoconductivity or photoemission processes occurs when the geometry of the excited state is most similar to the equilibrium geometry of the anionic defect. At bulk, the most probable transition energy for the photoemission process of a particular anionic defect is herein called  $VDE_{\infty}$  (vertical detachment energy at bulk; see Fig. 1) as it has only been determined in water by extrapolating the measured vertical detachment energies of hydrated electron<sup>9</sup> and hydrated iodide<sup>10,11</sup> clusters to bulk. The quantity  $VDE_{\infty}$  is related to the bulk photoemission threshold (PET) of the anionic defect, but in water these two quantities are significantly different. The PET corresponds to the minimal photon energy at which there is sufficient geometric overlap between initial and final states to detect signal, whereas  $VDE_{\infty}$  indicates optimal or most probable overlap.

If the electron is removed to vacuum from an anionic defect in a photoemission process, the newly created state finds itself in a configuration far from its minimum energy. The surrounding solvent molecules respond on different timescales (both in terms of their electronic polarization which is fast and their nuclear positions and molecular orientation which are much slower than the vertical excitation process) to a structure favorable to the resulting neutral radical, should it be stable. The magnitude of energy associated with this process is called the reorganization energy (RE). It is typically assigned a positive value, so RE is the reverse of the above-described reorientation process. The completely relaxed state that eventually results from the photoemission process is the vacuum level. The adiabatic reattachment of an electron to the vacuum level structure, regaining the original anionic defect, defines the defect's bulk adiabatic electron affinity,  $AEA_{\infty}$ , i.e., the aqueous bulk equivalent of the anion's gas phase adiabatic electron affinity. (This should not be confused with the property called the "liquid electron affinity" which is not a defect property.) The following energetic relation for the general defect,  $A$ , results

$$VDE_{\infty}(A^{-}) = RE + AEA_{\infty}(A). \quad (1)$$

The defect's  $AEA_{\infty}$  can be given (as depicted in Fig. 1) by a thermochemical cycle,

$$AEA_{\infty}(A) = \Delta E_{\text{sol}}(A) - \Delta E_{\text{sol}}(A^{-}) + AEA[A(g)], \quad (2)$$

where the  $\Delta E_{\text{sol}}$ 's are the solvation energies of the anionic defect  $A^{-}$  and its corresponding radical  $A$  (both of which are typically negative quantities), and  $AEA[A(g)]$  is the gas phase adiabatic electron affinity of  $A$  (conventionally positive if  $e^{-}$  attachment is stabilizing). The quantity  $AEA_{\infty}$  can also be related to the conduction band edge as

$$AEA_{\infty}(A) = -V_0 - \Delta E_{\text{defect}}(A), \quad (3)$$

where  $V_0$  is the energy to take a zero kinetic energy, gas phase electron into the condensed phase to the bottom of the conduction band as a delocalized conducting or quasi-free

TABLE I. Energetic location of defects beneath vacuum level and defect photoemission thresholds. All units are in eV.

Defect ( <i>A</i> )	$\Delta E_{\text{sol}}$ ( <i>A</i> <sup>-</sup> )	$\Delta E_{\text{sol}}$ ( <i>A</i> )	AEA [ <i>A</i> ( <i>g</i> )]	AEA <sub>∞</sub> <sup>f</sup>	PET [ <i>A</i> -( <i>aq</i> )]	VDE <sub>∞</sub> <sup>j</sup>
<i>e</i> <sup>-</sup>	-1.72 <sup>a</sup>	0.000	0.000	1.72	2.4 <sup>g</sup>	3.32 <sup>j</sup>
I <sup>-</sup>	-2.549 <sup>b</sup>	-0.03 <sup>c</sup>	3.063 <sup>c</sup>	5.58	7.19 <sup>h</sup>	8.06 <sup>k</sup>
Br <sup>-</sup>	-2.930 <sup>b</sup>	-0.16 <sup>c</sup>	3.363 <sup>c</sup>	6.13	8.05 <sup>h</sup>	NA
Cl <sup>-</sup>	-3.278 <sup>b</sup>	-0.19 <sup>c</sup>	3.613 <sup>c</sup>	6.70	8.81 <sup>h</sup>	NA
OH <sup>-</sup>	-4.970 <sup>b</sup>	-0.37 <sup>d</sup>	1.83 <sup>e</sup>	6.43	8.45 <sup>h</sup>	NA
H <sub>2</sub> O		-0.456 <sup>e</sup>			10.06 <sup>i</sup>	

<sup>a</sup>This work.<sup>b</sup>Reference 13.<sup>c</sup>Estimated in Sec. III from pairwise interactions with water, uncertainty  $\approx \pm 0.1$  eV.<sup>d</sup>Calculated in Sec. V.<sup>e</sup>Reference 12.<sup>f</sup>Equation (2).<sup>g</sup>New estimate based on this work's small  $V_0$  value of water.<sup>h</sup>Reference 16.<sup>i</sup>Reference 15.<sup>j</sup>Reference 9.<sup>k</sup>Reference 11.

electron, and  $\Delta E_{\text{defect}}(A)$  is the energy to localize a conducting electron in water onto the neutral radical *A*. Both  $V_0$  and  $\Delta E_{\text{defect}}(A)$  are typically negative quantities as represented in Fig. 1. Note that the initial and final states for the two processes,  $\Delta E_{\text{defect}}$  and RE (see Fig. 1), involve the same geometric differences in solvent structure, so RE is one component of  $\Delta E_{\text{defect}}$  which additionally includes charge stabilization upon the solvated radical *A*. Therefore, the magnitude of  $\Delta E_{\text{defect}}$  should always be greater than RE for defects that energetically prefer to be negatively charged (electrons or anions).

## B. The need to consider reorganization energy in water

Anionic defect states can be readily located beneath the vacuum level by  $\text{AEA}_{\infty}$  using Eq. (2) and knowledge of  $\Delta E_{\text{sol}}(A)$ ,  $\Delta E_{\text{sol}}(A)$ , and  $\text{AEA}[A(g)]$ . These quantities,<sup>12–14</sup> PETs,<sup>15–19</sup> and VDEs<sup>9–11</sup> can be found in Table I for the *e*<sup>-</sup>, I<sup>-</sup>, Br<sup>-</sup>, Cl<sup>-</sup>, and OH<sup>-</sup> defects. The radical solvation energies,  $\Delta E_{\text{sol}}(A)$ , are the least well-known of these quantities, but they are also much smaller than the other terms. The radical solvation energies have been estimated using low level *ab initio* methods<sup>20</sup> (UHF/3-21G) to determine energy changes of -0.23, -0.19, -0.03, -0.52, and -0.48 eV for the reaction of  $A + \text{H}_2\text{O} \rightarrow A(\text{H}_2\text{O})$  where  $A = \text{Cl}, \text{Br}, \text{I}, \text{OH},$  and  $\text{H}_2\text{O}$ , respectively. Note that each of these interactions is favorable, so bulk solvation energies can be expected to be stabilizing for the halogen radicals, but weaker than that of OH and H<sub>2</sub>O. The fraction of the single water binding energies of Cl, Br, and I relative to that of OH and H<sub>2</sub>O is used as a scaling factor with the bulk solvation energies of OH (as determined in Sec. V) and H<sub>2</sub>O to estimate the bulk values for Cl, Br, and I. The average of the result scaled from OH and H<sub>2</sub>O is shown in Table I. We expect these values to be accurate within about 0.1 eV.

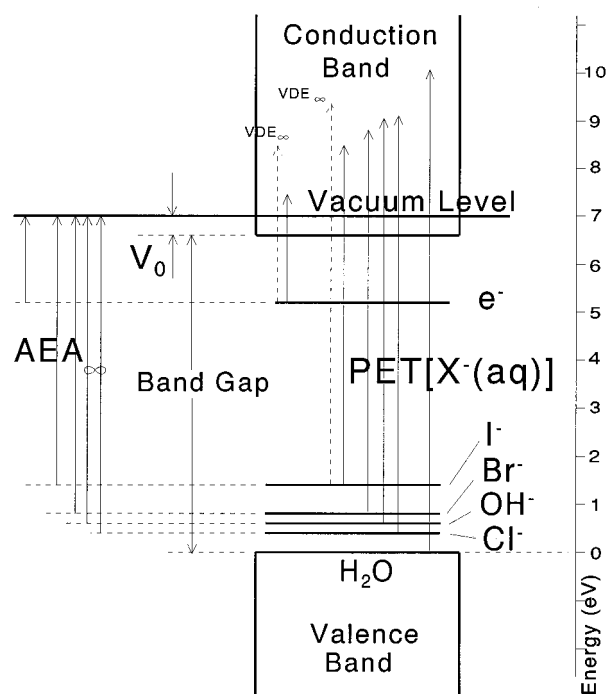


FIG. 2. Photoemission thresholds (PETs) of various anionic defects, including the hydrated electron, are plotted on a typical band energy diagram of water. The anionic defect states are located relative to the vacuum level by the quantity  $\text{AEA}_{\infty}$  using Eq. (2) and the data in Table I. All of the PETs access the conduction band at different energies which are well above the vacuum level. The deeper into the band gap a defect lies, the higher the energetic access into the conduction band, showing that it is important to explicitly consider solvent reorientation about charge. Also shown are the vertical detachment energies ( $\text{VDE}_{\infty}$ , i.e., most probable transition energy) for the hydrated electron and iodide defects. Clearly they are not equal to the PETs and extend  $\sim 1$  eV further into the conduction band providing more evidence for the need to consider solvent reorganization energy (RE).

In Fig. 2, the experimental PETs of various anionic defects including the hydrated electron are drawn from their defect state locations beneath the vacuum level. Note that the PET of the hydrated electron has not yet been measured at bulk and is a quantity derived from present considerations. If there was nothing unusual about water (or, to be more precise, if there was sufficient optical access to the vacuum level), then all of the PETs would access the same energy in the conduction band defining the vacuum level. However, all of the PETs access the conduction band at different points, well above the vacuum level (which must lie at or below the lowest PET access point). Notice that (1) the thresholds are not determined by the vacuum level, and that (2) the deeper into the band gap a defect lies, the higher the energetic access into the conduction band. These observations suggest that the PETs are primarily governed by the lack of geometric overlap between the initial state (where solvent molecules near the charge align their dipoles to the charge) and the final state (which is uncharged and would not prefer dipole aligned solvent configurations). Clearly it is very important to consider reorganization energy (RE); i.e., RE cannot be considered to be approximately zero. Whenever RE is important, it follows that  $\text{VDE}_{\infty}(A^-)$  will not be equivalent to the

PET[ $A^-(aq)$ ] and aqueous energetic diagrams (such as Fig. 2) require more degrees of freedom to account for RE (in a manner analogous to a molecular potential energy surface). There are now determinations of  $VDE_\infty(A^-)$  from negative ion photoelectron spectroscopic studies<sup>9–11</sup> of hydrated electron and iodide clusters which show that most-probable vertical access extends about 1.0 eV further into the conduction band than the PETs (as depicted with dotted lines in Fig. 2). These  $VDE_\infty$  values determine REs [by Eqs. (1) and (2)] for  $e^-(aq)$  and  $I^-(aq)$  of 1.60 and 2.5 eV, respectively. Therefore, the PETs provide only minimal estimates of REs which are about 1 eV shy of the true RE values. This observation, when considered in the appropriate terms for the photoionization process, explains why the present determination of  $V_0$  is different from many experimental literature values<sup>21,22</sup> by about 1 eV.

## II. RESULTS

### A. Determination of $V_0$

The band gap, which defines the energy difference between the valence band edge (top of the valence band) and the conduction band edge (bottom of the conduction band), is defined relative to the vacuum level by the quantity  $V_0$  (which is sometimes also called the liquid electron affinity). The energy to promote a delocalized, conducting electron of minimal energy into vacuum with zero kinetic energy is  $-V_0$ . The top of the band gap (conduction band edge) cannot yet be placed accurately on the diagram in Fig. 2, because its exact location depends on the value of  $V_0$ . Since it should not be placed above any of the PETs or below a defect, the hydrated electron data provide the tightest constraints in this regard.

The hydrated electron species also provides a very useful simplification of the schematics in Fig. 1. Since the defect,  $A^-$ , is an electron, and there is no corresponding radical,  $A$ , to provide a solvent orientation different from that of pure water, one finds that  $AEA[e^-(g)] = \Delta E_{sol}(A) = 0$  and  $AEA_\infty(e^-) = -\Delta E_{sol}(e^-)$  for the electron defect. A simplified schematic of the hydrated electron case is provided in Fig. 3. The Bowen group's detachment work<sup>9</sup> gives  $VDE_\infty(e^-) = 3.32$  eV, and crossed electron and water cluster beam experiments of Knapp *et al.*<sup>23</sup> show that  $(H_2O)_{11}$  has a small but positive adiabatic electron affinity,  $AEA_{11} \approx 0.0$  eV. The Bowen group's experiments also show that the VDEs of hydrated electron clusters progress to bulk with the continuum, dielectric sphere  $n^{-1/3}$  slope of 5.73 eV. It has been shown<sup>11</sup> that there is a constant ratio (0.643) between the continuum dielectric sphere  $n^{-1/3}$  slope of cluster solvation enthalpies and the cluster vertical detachment energies ( $VDE_n$ 's). Since in the special case of the hydrated electron, the solvation enthalpy and adiabatic electron affinity are the same, it follows that the cluster  $AEA_n$  values must also progress to bulk with the continuum, room temperature, dielectric sphere value of  $\sim 3.83$  eV for solvation enthalpy.<sup>11</sup> Extrapolation of the  $AEA_{11}$  value of zero to bulk with the continuum dielectric sphere slope results in  $AEA_\infty = 1.72 \pm 0.05$  eV. This value is consistent with the ac-

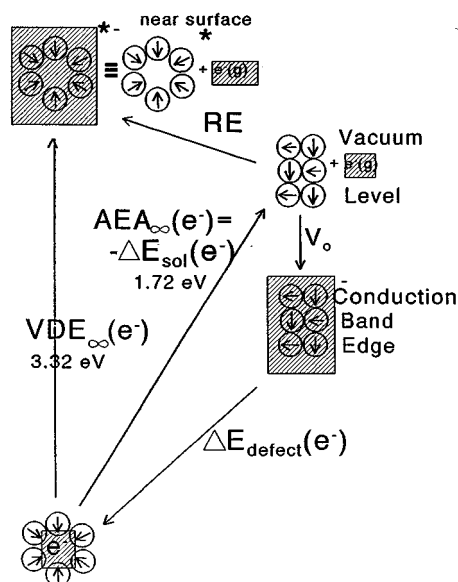


FIG. 3. Pictorial representation of the energetics when the anionic defect is the hydrated electron. This particular defect simplifies the picture presented in Fig. 1 because there is no corresponding radical ( $A$ ) for the electron to localize upon. The values for  $VDE_\infty$  and  $AEA_\infty$  come from experimental studies of large hydrated electron clusters [Refs. 9 and 23] and are used to determine a reorganization energy (RE) of 1.6 eV for aqueous electron solvation. The value of RE represents a minimum contribution to the value of  $\Delta E_{defect}(e^-)$  and consequently an upper limit to the magnitude of  $V_0$ , the liquid electron affinity of water.

cepted estimate of the electron's solvation enthalpy<sup>24</sup> based on its absorption spectrum. By Eq. (1), the solvent reorganization energy for the electron,  $RE(e^-)$ , is 1.60 eV.

As has already been observed, the initial and final states for the two processes,  $\Delta E_{defect}$  and RE (see Fig. 1 or 3) involve the same geometric differences in solvent structure, so RE is one component of  $\Delta E_{defect}$  which additionally includes charge stabilization (expected to be favorable for defects that prefer to be negatively charged). The RE associated with the hydrated electron represents a minimum magnitude for  $\Delta E_{defect}(e^-)$ , so  $-\Delta E_{defect} \geq RE$ . Using this inequality and Eq. (3) solved for  $V_0$ , one finds that  $V_0 = -\Delta E_{defect} - AEA_\infty \geq RE - AEA_\infty = 1.60$  eV  $- 1.72$  eV =  $-0.12$  eV. Therefore,  $V_0 \geq -0.12$  eV. The value of  $V_0$  in a liquid is governed by two properties: the degree of long-range order in the liquid<sup>25</sup> and its polarizability.<sup>26</sup> A liquid with molecules arranged symmetrically on average will be more capable of accommodating a low energy, Bloch-like wave function for the quasi-free electron than one with molecules arranged in a disorderly fashion. Since liquids with a high degree of long-range order have negative values of  $V_0$ ,<sup>25</sup> water (with long range structure dictated by hydrogen bonding) can be expected to have a negative value of  $V_0$ , shrinking the range of possible values to  $-0.12$  eV  $\leq V_0 \leq 0.0$  eV.

An important discussion and review on the value of  $V_0$  has been given by Han and Bartels.<sup>27</sup> The present determination is consistent with Jortner's theoretical considerations<sup>26</sup>  $-0.5 < V_0 < 1.0$ , quite close to Henglein's<sup>28,29</sup> calculations of  $-0.2$  eV, but in disagreement with the accepted

value for  $V_0$  of  $-1.2 \pm 0.1$  eV deduced by Grand, Bernas, and Amouyal<sup>21</sup> from photoionization measurements on indole and other experimental methods.<sup>22,30–34</sup> The considerations in Sec. III (about the need to consider reorganization energy) apply equally well to photoionization as to photoemission. The authors of the indole work considered the possible difference between the vertical ionization potential and the measured photoionization threshold [see their Eq. (1')], but assumed it could be ignored. This difference (between the most probable transition energy and the threshold) is now known to be about 1 eV in the photoemission of the  $1^-(aq)$  and  $e^-(aq)$  defects (from the cluster extrapolated values) and probably the same in the photoionization of aqueous indole; i.e., the effect cannot be ignored.

As the lower limit of  $V_0$  introduced here is an order of magnitude less negative than the most commonly referenced, experimental value of  $-1.2$  eV,<sup>21</sup> some justification is offered to show that the new, smaller value is reasonable. While long-range order may determine whether  $V_0$  is negative, the magnitude of  $V_0$  depends on the polarizability of the liquid. Generally, the greater the polarizability, the more negative  $V_0$  tends to be. Thus it is instructive to compare the presently determined  $V_0$  of water to directly measured  $V_0$  values of liquids with high degrees of long-range order and polarizabilities similar to water. Given the optical polarizability of water<sup>35,36</sup> ( $\alpha_{M,optical} = 3.70$  cm<sup>3</sup> mol<sup>-1</sup>), two liquids with comparable polarizabilities are cryogenic methane<sup>37</sup> ( $\alpha_{M,static} = 6.7$  cm<sup>3</sup> mol<sup>-1</sup>) and cryogenic argon<sup>38</sup> ( $\alpha_{M,static} = 4.06$  cm<sup>3</sup> mol<sup>-1</sup>). The appropriate polarizability for comparison in water is the optical polarizability (rather than static) because the quasi-free electron state lasts only as long as the water molecules do not reorient (or produce the appropriate fluctuation) to begin formation of the hydrated electron trap; hence, only the electronic component of the polarizability, and not dipole reorientation, is needed to describe the interaction between a quasi-free electron and water. The distinction between optical and static polarizabilities is not an issue with methane or argon because they do not have dipoles which can energetically favor a particular orientation about charge. Because of the spherical shapes of the CH<sub>4</sub> molecules and Ar atoms, these moieties will tend to stack themselves in a symmetric fashion in the liquid phase, guaranteeing a high degree of long-range order. However, the measurement of  $V_0$  for liquid methane and argon is clearly not complicated by solvent reorganization energy. Two published values of  $V_0$  for methane are  $-0.18$  eV<sup>25</sup> and  $-0.25$  eV.<sup>39</sup> A  $V_0$  value of  $-0.21$  eV<sup>25</sup> has been reported for argon. As suggested by the polarizabilities, the presently determined lower limit for water ( $V_0 = -0.12$  eV) is a bit less negative than the  $V_0$  values of comparable liquids. This value is much more consistent with the  $V_0$  values of comparable liquids than the commonly referenced value<sup>22,30–34</sup> of about  $-1.2$  eV. The problem of  $V_0$  in water would appear to be a very important and challenging one, meriting contemporary theoretical consideration.

TABLE II. Solvation energies of  $X=H_2O$  and OH in water clusters,  $X + (H_2O)_n \rightarrow X(H_2O)_n$ . All units are eV.

$n$	$H_2O^a$	OH
1	-0.152	-0.360
2	-0.285	-0.335
3	-0.359	-0.299
4	-0.238	-0.286
5	-0.277	-0.225
6	-0.288	-0.146
7	-0.497	-0.372
8	-0.143	0.035
9	-0.454	-0.324
10	-0.175	-0.021
11	-0.746	-0.389
12	-0.011	-0.004
13	-0.306	-0.087
14	-0.222	-0.119
15	-0.509	-0.282

<sup>a</sup>Reference 43.

## B. Determination of the solvation energy of the OH radical

The other big unknown in the determination of the band gap of water is the solvation energy of the OH radical,  $\Delta E_{sol,n}(OH)$ . To determine this quantity semiempirical MNDO-type calculations with the PM3 parameterization<sup>40,41</sup> have been performed using the HyperChem software package<sup>42</sup> to find the global minimum energies of  $OH(H_2O)_{n=0-15}$  clusters and  $(H_2O)_{n=1-15}$  clusters. The minimum energy water cluster structures were in exact agreement with the structures and energies published<sup>43</sup> in 1993 by Vasilyev. This work captured many of the important features that are now emerging about water clusters.<sup>44–49</sup> There is a transition from ring structures to more condensed structures at  $n=6$  as is seen in both *ab initio*<sup>50</sup> and experimental work<sup>51</sup> and a family of particularly stable stacked cube structures at  $n=8, 12, 16$  which have been investigated at  $n=8$  by both *ab initio*<sup>52</sup> and experimental<sup>53</sup> methods. The PM3 atomic binding energies ( $E$ ) were used to determine cluster solvation energies for the OH radical and a water molecule in water clusters as a function of cluster size,  $n$ , as follows:

$$X + (H_2O)_n \rightarrow X(H_2O)_n; \Delta E_{sol,n} = E[X(H_2O)_n] - E[(H_2O)_n] - E[X]. \quad (4)$$

The cluster solvation energies are presented in Table II and Fig. 4.

In the small cluster regime there are large oscillations (this is not noise) in the solvation energy because the minimum energy structure is jumping from one family of structures to another with each increasing step in cluster size. For instance, there exists a family of stacked cube structures<sup>43</sup> for  $(H_2O)_{n=8,12,16,\dots}$  which are particularly stable, so when a single water molecule is solvated by 7, 11, or 15 other water molecules, larger magnitudes of solvation energy are obtained. The cluster solvation data for  $H_2O$  in  $(H_2O)_n$  roughly follows a continuum relation,<sup>54</sup> which is based on the tem-

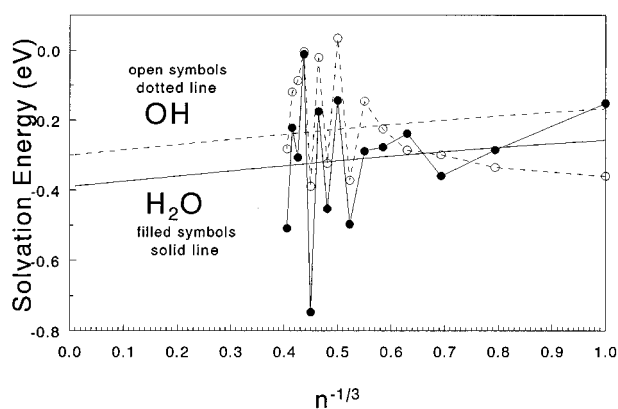


FIG. 4. PM3 calculated solvation energies of OH radical and a water molecule in water clusters vs  $n^{-1/3}$ , where  $n$  is the number of solvating waters in the cluster. The OH radical data are plotted with open symbols and dotted lines. The  $\text{H}_2\text{O}$  data are plotted with filled symbols and solid lines. Each data set has been fit to a continuum relation based on bulk surface tension data, spherical water droplets, and converting the droplet radius into a relation for the number of solvating water molecules as given in Eq. (5) and Ref. 54. A value of  $-0.39 \pm 0.05$  eV was determined for the solvation energy of a water molecule which is only 0.07 eV different than the negative of the heat of vaporization of water. A value of  $-0.30 \pm 0.04$  eV was determined for the bulk solvation energy of the OH radical which is revised to  $-0.37$  eV by consideration of the offset in the process for water. The uncertainties indicate the statistical uncertainty ( $1\sigma$ ) of the fitting procedure, not the absolute accuracy of the values.

perature dependence of the difference in the chemical potential (a function of surface tension and radius) of different sized spherical drops (producing the constant,<sup>55</sup> 0.226 eV, seen below). Here it is given in terms of the number of solvating water molecules ( $n$ ) instead of the droplet radius:

$$\Delta E_{\text{sol},n} = (0.226 \text{ eV})[(n+1)^{2/3} - n^{2/3}] + \Delta E_{\text{sol},\infty}, \quad (5)$$

where  $\Delta E_{\text{sol},\infty}$  is determined by the method of least squares. A value of  $-0.39 \pm 0.05$  eV is obtained for  $\Delta E_{\text{sol},\infty}[\text{H}_2\text{O}]$  which is shy of  $-\Delta H_{\text{vap}}(\text{H}_2\text{O}) = -0.456$  eV<sup>12</sup> in magnitude by only 0.07 eV. The best fit curve for solvation of a water molecule [from Eq. (5)] is shown in Fig. 4 as a solid line with the filled symbols.

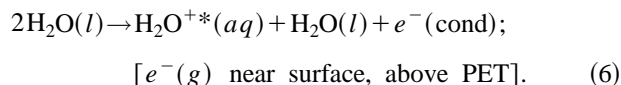
As  $\text{OH}(\text{H}_2\text{O})_n$  clusters get large, the energetics of adding another water molecule (at the surface, nearby other water molecules) will not be much affected by the details of the neutral radical solvation on the inside. The solvation energetics will eventually progress to bulk in the same manner as the solvation of a water molecule in water clusters, i.e., governed by the surface tension of bulk water. Most all of the difference in solvation that an OH radical will experience as compared to a water molecule will occur in the small cluster size regime. So the  $\text{OH}(\text{H}_2\text{O})_n$  solvation data are fit (i.e., extrapolated to bulk) with the same functional form as the water data [Eq. (5)], and provide a solvation energy for the hydroxyl radical ( $\Delta E_{\text{sol},\infty}[\text{OH}]$ ) of  $-0.30 \pm 0.04$  eV. The best fit curve for solvation of the OH radical [from Eq. (5)] is shown in Fig. 4 as a dotted line with the open symbols. Since the method applied to water was 0.07 eV shy in the magnitude of the bulk solvation enthalpy, we add a similar offset to the fitted value for OH to obtain  $\Delta E_{\text{sol},\infty}[\text{OH}] = -0.37$  eV.

This value is in good accord with the experimental determination<sup>56</sup> of  $\Delta G_{\text{sol},\infty}[\text{OH}] = -0.10$  eV. The difference of  $-0.27$  eV is approximately  $T\Delta S$  for hydration of  $\text{OH}(g)$  which would be expected to be a bit smaller in magnitude than the  $-0.367$  eV value<sup>12</sup> of  $T\Delta S$  for hydration of  $\text{H}_2\text{O}(g)$ .

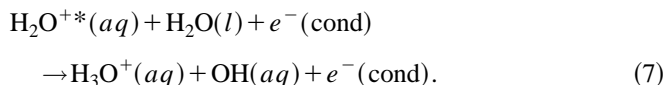
### III. INCORPORATION INTO AN OVERALL PICTURE OF WATER

#### A. The chemical identity of the conduction band edge

The valence band edge of liquid water can be chemically described as  $\text{H}_2\text{O}(l)$ . Vertical photoionization of an  $\text{H}_2\text{O}$  molecule in liquid water produces a delocalized (quasi-free or conducting) electron and an  $\text{H}_2\text{O}^+$  ion with the geometry of a neutral, liquid water molecule. If this process happens near the surface at an energy above the PET, the conducting electron can be emitted into vacuum:



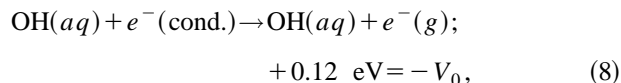
The  $\text{H}_2\text{O}^+$  is unstable and attacks<sup>4,27,57,58</sup> a nearby water producing  $\text{H}_3\text{O}^+$  and OH, hence the requirement for two water molecules in order to chemically identify the various states related to the band gap of water. The bottom of the conduction band is associated with complete relaxation of solvating water about the  $\text{H}_3\text{O}^+$  and OH moieties and equilibration with the delocalized electron.



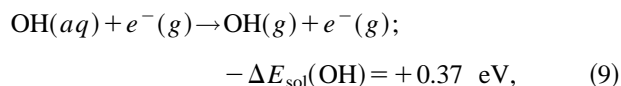
The absence of localized charged species in the valence band edge [ $2\text{H}_2\text{O}(l)$ ] stands in contrast to the conduction band edge [ $\text{H}_3\text{O}^+(aq) + \text{OH}(aq) + e^-(\text{cond})$ ] producing a big difference in solvent orientation. Solvent molecules reorient about the  $\text{H}_3\text{O}^+$  defect (and to a lesser extent about OH) compared to the structure of pure water, making the conduction band edge vertically inaccessible from the valence band edge. Consequently, there can be no direct optical measurement of the band gap of water.

#### B. The band gap by location of the $\text{OH}^-$ defect state

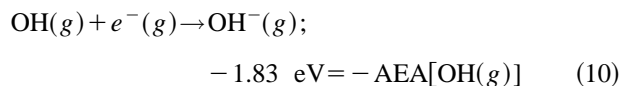
To preserve chemical and charge balance with the chemical identity of the conduction band edge, the  $\text{OH}^-$  defect state is identified as  $\text{H}_3\text{O}^+(aq) + \text{OH}^-(aq)$ . It is reasonable to call it the  $\text{OH}^-$  defect state because the  $\text{H}_3\text{O}^+(aq)$  entity is shared with the conduction band edge. The  $\text{OH}^-$  defect state is energetically placed relative to the conduction band edge by  $V_0 - \Delta E_{\text{sol}}(A) + \Delta E_{\text{sol}}(A^-) - \text{AEA}[A(g)]$ . To get from the conduction band edge to the  $\text{OH}^-$  defect state involves the following reactions:



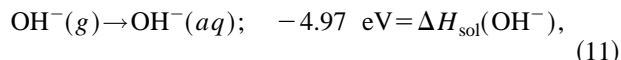
(this work, Ref. 59)



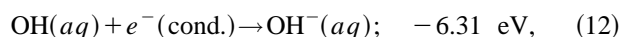
(this work)



(Ref. 12)



(Ref. 13) which sum to



where the correction of Eq. (11) from an enthalpy to an internal energy has been ignored. The  $\text{OH}^-$  defect state can also be placed relative to the valence band edge by



(Ref. 60). The band gap energy is the difference between Eqs. (13) and (12) which is 6.89 eV (assuming  $V_0 = -0.12 \text{ eV}$ ). Literature values for the band gap of water<sup>21,27</sup> seem to range from 6.5 to 9.0 eV. The lowest values derive from the photoionization thresholds for observing the hydrated electron upon irradiation of water with 7.8 eV<sup>8</sup> (showing exponential photon energy dependence), 6.8 eV<sup>61</sup> and 6.5 eV photons.<sup>62</sup> If this process involves the conduction band, then these values are upper limits for the band gap of water. However, considering the 10-eV photoemission threshold of water<sup>15</sup> and the large role of reorganization energy in the vertical excitation process, the participation of the conduction band in this interesting process (at least in a simple way allowing the band gap to be characterized) is not evident.<sup>63</sup> There is an electronic calculation<sup>64</sup> of 7.8 eV for the spacing of the highest occupied electronic level and the lowest unoccupied valence state in cubic ice, but this technique was not used to approach the conduction band. A simple polarization model<sup>21</sup> produced an estimate of the band gap of 7.0 eV, but this calculation employed a value of  $V_0$  equal to  $-1.2 \text{ eV}$ . Using the presently determined  $V_0$  value, a band gap of 8.1 eV would have been obtained. There are also x-ray photoelectron investigations<sup>65-67</sup> on ice characterizing the sum of the band gap and  $V_0$  value as ranging from 8.7 to 9.0 eV which, in view of the presently developed constraints, provide an upper limit for the band gap of  $\sim 8.6 \text{ eV}$ . It has been a common practice in the literature to place the vacuum level using the PET of water<sup>8,68</sup> defining what could be called a ‘‘vertical’’ vacuum level. The bottom of the conduction band is then placed by the magnitude of  $V_0$  below the vacuum level. Using typical literature values (PET[ $\text{H}_2\text{O}$ ]=10.06 eV<sup>15</sup> and  $V_0 = -1.2 \text{ eV}$ <sup>21</sup>), this approach defines a band gap of 8.9 eV. So the current determination of 6.9 eV for the band gap of water is significantly smaller than the common expectation, presenting a significantly different picture of water photophysics.

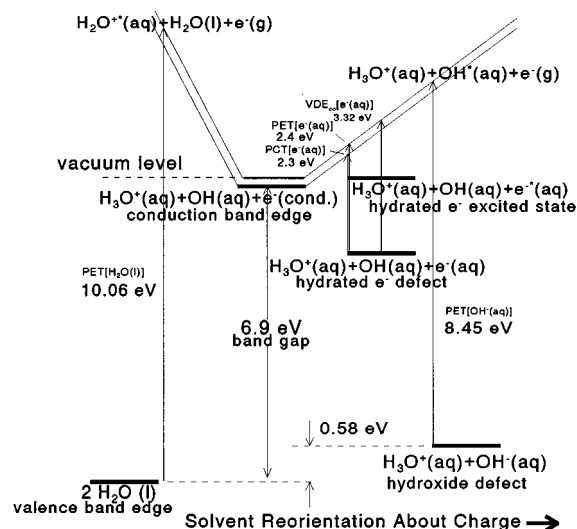


FIG. 5. Energy diagram for bulk water which incorporates the effect of reorientation of solvating water molecules about charge (adiabatic polarization). This presentation clearly distinguishes between the adiabatic and vertical properties of water as an amorphous semiconductor. Particularly noteworthy are the small values of the liquid electron affinity (difference between the vacuum level and the conduction band edge,  $-0.12 \text{ eV} \leq V_0 \leq 0 \text{ eV}$ ) and band gap (6.9 eV) that have been determined.

### C. Energy diagram for bulk water

The above considerations concerning the band gap, conduction band edge, and vacuum level are summarized in the energy diagram for bulk water in Fig. 5. Simple band pictures for bulk water<sup>6</sup> (an insulator, i.e., a large band gap semiconductor) consist of a completely filled valence band separated from the bottom of the conduction band by a large band gap which may be occupied by various defect states (see Fig. 2). It is typical of such diagrams to ignore the nature of the oppositely charged counterpart to the charged defect state of interest, as its presence is implied by the assumed neutrality of the bulk material. So in Fig. 5, the full charge and mass conserved chemical identities are given for each level. Notice that the conduction band edge corresponds<sup>27</sup> to  $\text{H}_3\text{O}^+(aq) + \text{OH}(aq) + e^-(\text{cond.})$ . Simple band diagrams also have nothing to indicate the geometric structure of the states involved (as potential energy surfaces might for a gas phase diatomic molecule or band energies vs  $\mathbf{k}$  vector for crystals). Since reorganization energy is so important in water, it has been included in a crude and schematic fashion as the  $x$  axis in the energy level diagram for pure water in Fig. 5. The left hand side of this diagram represents water in its neutral state with no reorientation about charge (top of the valence band of water), while the right side represents reorganization about two ions,  $\text{H}_3\text{O}^+(aq) + \text{OH}^-(aq)$ , with large solvation energies (common defect state). The middle of the diagram is for water which has reoriented about one strongly solvated ion,  $\text{H}_3\text{O}^+(aq)$ , as in the conduction band edge. The lateral width of each energy level crudely represents the range of geometric structures sampled at room temperature. The hydrated electron defect state is associated with a modest reorganization of water

about the electron, so it is placed in the intermediate region between one and two strongly solvated ions. Note that this diagram also depicts a separate space for the electronically excited ( $p$ -state) hydrated electron even though this level lies above the minimum energy of the conduction band. It is easy to imagine how the higher levels of this state communicate with the conduction band (while the lower levels do not) producing the blue, asymmetric tail to the absorption spectrum of the hydrated electron.<sup>24,69</sup>

In Fig. 5, it is evident that the band gap of water can not be determined with a vertical transition; hence no experiment has succeeded in directly measuring this property. On this diagram, the four upwardly directed arrows from the edge of their state levels represent vertical, experimentally observed thresholds, including the photoemission threshold from pure water<sup>15</sup> ( $\text{PET}[\text{H}_2\text{O}(l)] = 10.06$  eV), the photoemission threshold<sup>16–19</sup> from hydroxide in water ( $\text{PET}[\text{OH}^-(aq)] = 8.45$  eV), the photoconductivity threshold<sup>70</sup> of hydrated electrons in ice ( $\text{PCT}[e^-(\text{ice})] = 2.3$  eV), and the photoemission threshold of hydrated electrons in water ( $\text{PET}[e^-(aq)] \approx \text{PCT}[e^-(\text{ice})] - V_0 = 2.4$  eV). None of these PETs accesses the conduction band at the vacuum level which has been placed  $\sim 0.1$  eV above the conduction band edge by our preferred value<sup>59</sup> of  $\sim -0.1$  eV for  $V_0$ . Note that a vertical transition, such as  $\text{VDE}_\infty$  for the hydrated electron defect, is drawn from the center of the defect's level because this property represents the most probable transition energy. It would certainly not access the conduction band at the same place as the corresponding PET which represents the threshold for detectable signal.

#### IV. DISCUSSION

As illustrated in Fig. 2, the PETs of pure water and its anionic defects do not determine the vacuum level of water. In water, PETs are instead governed by the availability of sufficient geometric overlap (of solvent configurations about charged initial defect states and noncharged product states) for signal to be detected. There is almost no chance of accessing the bottom of the conduction band of water in a photoemission process. Since solvent polarization is the critical factor, it would be worthwhile to examine the effect of solvent polarization on the empirical photoemission threshold laws which are used to determine PET values. Threshold laws in water are likely to differ from the more familiar case of measurable vertical access to the conduction band at the energy of the vacuum level. Experimental photoemission thresholds in water are likely to be very difficult to discern.

Relative to the top of the valence band of water, the currently determined energetic position for the bottom of the conduction band is  $\sim 2$  eV lower than what is often presented in the literature.<sup>8,68</sup> Consequently, states producing most of the Urbach tail or exponential edge in the vacuum ultraviolet absorption<sup>71,72</sup> and photoionization<sup>8</sup> spectra of water (photon energies from 6.9 to 9 eV) do not lie below the conduction band edge. It becomes important to reconsider the role of both electron-trapping states and conduction band

states with regard to solvent polarization in this spectral region.

The various PETs shown in Fig. 5 serve to map the contour of the conduction band as a function of solvent re-orientation about charge. The shape of the conduction band in Fig. 5 is reminiscent of a molecular excited state potential energy surface. It suggests that a quantitative treatment of water's conduction band structure/potential surface might be gainfully approached as a function of solvent polarization. The energy level diagram in Fig. 5 concisely summarizes much of the information that has been deduced in this work. We conclude by noting that cluster studies are certainly contributing to a better understanding of water.

#### ACKNOWLEDGMENTS

J.C. (CHE-9528977) and K.B. (CHE-9007445) thank the National Science Foundation for support of this work. We also thank S. Singer, S. T. Arnold, J. G. Eaton, and T. Tuttle for their discussions and input.

- <sup>1</sup> S. T. Arnold, J. V. Coe, J. G. Eaton, C. B. Freidhoff, L. Kidder, G. H. Lee, M. R. Manaa, K. M. McHugh, D. Patel-Misra, H. W. Sarkas, J. T. Snodgrass, and K. H. Bowen, in *The Chemical Physics of Atomic and Molecular Clusters*, edited by G. Scoles (North-Holland, Amsterdam, 1990).
- <sup>2</sup> G. Markovich, R. Giniger, M. Levin, and O. Cheshnovsky, *J. Chem. Phys.* **95**, 9416 (1991).
- <sup>3</sup> K. Liu, J. D. Cruzan, and R. J. Saykally, *Science* **271**, 929 (1996).
- <sup>4</sup> M. Ahmed, C. J. Apps, C. Hughes, and J. C. Whitehead, *J. Phys. Chem.* **98**, 12 530 (1994).
- <sup>5</sup> T. Schindler, C. Berg, G. Niedner-Schatteburg, and V. E. Bondybey, *Chem. Phys. Lett.* **250**, 301 (1996).
- <sup>6</sup> F. Williams, S. P. Varma, and S. Hillenius, *J. Chem. Phys.* **64**, 1549 (1976).
- <sup>7</sup> M. Szklarczyk, R. C. Kainthla, J. O'M. Bockris, *J. Electrochem. Soc.* **136**, 2512 (1989); see Fig. 17 after T. Watanabe and H. Gerischer, *J. Electroanal. Chem.* **122**, 73 (1981).
- <sup>8</sup> T. Goulet, A. Bernas, C. Ferradini, and J.-P. Jay-Gerin, *Chem. Phys. Lett.* **170**, 492 (1990).
- <sup>9</sup> J. V. Coe, G. H. Lee, J. G. Eaton, S. T. Arnold, H. W. Sarkas, K. H. Bowen, C. Ludewigt, H. Haberland, and D. R. Worsnop, *J. Chem. Phys.* **92**, 3980 (1990).
- <sup>10</sup> G. Markovich, S. Pollack, R. Giniger, and O. Cheshnovsky, *J. Chem. Phys.* **101**, 9344 (1994).
- <sup>11</sup> J. V. Coe, *J. Phys. Chem. A* **101**, 2055 (1997).
- <sup>12</sup> R. C. Weast, Ed., *CRC Handbook of Chemistry and Physics*, 66th ed. (CRC, Boca Raton, 1985).
- <sup>13</sup> J. V. Coe, *Chem. Phys. Lett.* **229**, 161 (1994).
- <sup>14</sup> M. D. Tissandier, K. A. Cowen, W. Y. Feng, E. Gundlach, M. H. Cohen, A. D. Earhart, and J. V. Coe, *J. Phys. Chem.* (submitted).
- <sup>15</sup> P. Delahay and K. Von Burg, *Chem. Phys. Lett.* **83**, 250 (1981).
- <sup>16</sup> P. Delahay, *Acc. Chem. Res.* **15**, 40 (1982).
- <sup>17</sup> I. Watanabe, J. B. Flanagan, and P. Delahay, *J. Chem. Phys.* **73**, 2057 (1980).
- <sup>18</sup> P. Delahay and A. Dziedzic, *J. Chem. Phys.* **80**, 5381 (1984).
- <sup>19</sup> P. Delahay and A. Dziedzic, *Chem. Phys. Lett.* **108**, 169 (1984).
- <sup>20</sup> M. J. Frisch, G. W. Trucks, H. B. Schlegel, P. M. W. Gill, B. G. Johnson, M. A. Robb, J. R. Cheeseman, T. Keith, G. A. Peterson, J. A. Montgomery, K. Raghavachari, M. A. Al-Laham, V. G. Zakrzewski, J. V. Ortiz, J. B. Foresman, E. S. Replogle, R. Gomperts, R. L. Martin, D. J. Fox, J. S. Binkley, D. J. Defrees, J. Baker, J. P. Stewart, M. Head-Gordon, C. Gonzalez, and J. A. Pople, *GAUSSIAN 94*, Revision B.2, Gaussian Inc., Pittsburgh, PA, 1995; this small basis set is the biggest available in *GAUSSIAN 94W* which goes up to iodine.
- <sup>21</sup> D. Grand, A. Bernas, and E. Amouyal, *Chem. Phys.* **44**, 73 (1979).
- <sup>22</sup> R. E. Ballard, *Chem. Phys. Lett.* **16**, 300 (1972).



- <sup>23</sup>M. Knapp, O. Echt, D. Kreise, and E. Recknagel, *J. Chem. Phys.* **85**, 636 (1986).
- <sup>24</sup>E. J. Hart and M. Anbar, *The Hydrated Electron* (Wiley-Interscience, New York, 1970).
- <sup>25</sup>W. F. Schmidt, *Can. J. Chem.* **55**, 2197 (1977).
- <sup>26</sup>J. Jortner, *Ber. Bunsenges. Phys. Chem.* **75**, 696 (1971).
- <sup>27</sup>P. Han and D. M. Bartels, *J. Phys. Chem.* **94**, 5824 (1990); p. 5828 has a background on water photophysics.
- <sup>28</sup>A. Henglein, *Ber. Bunsenges. Phys. Chem.* **78**, 1078 (1975).
- <sup>29</sup>A. Henglein, *Can. J. Chem.* **55**, 2112 (1977).
- <sup>30</sup>Yu V. Pleskov and Z. A. Rottenberg, *J. Electroanal. Chem.* **20**, 1 (1969).
- <sup>31</sup>G. C. Barker, *Ber. Bunsenges. Phys. Chem.* **75**, 728 (1971).
- <sup>32</sup>A. M. Brodsky and Yu V. Pleskov, *Prog. Surface Sci.* **2**, 1 (1972).
- <sup>33</sup>K. Yamashita and H. Imai, *Bull. Soc. Chim. Jpn.* **45**, 628 (1972).
- <sup>34</sup>J. K. Sass and H. Gerischer, in *Photoemission and the Electronic Properties of Surfaces*, edited by B. Feuerbacher, B. Fitton, and R. F. Willis (Wiley-Interscience, New York, 1978).
- <sup>35</sup>P. Lorrain and D. Corson, *Electromagnetic Fields and Waves*, 2nd ed. (W. H. Freeman, San Francisco, 1970), pp. 115–116.
- <sup>36</sup>Molar polarizabilities were calculated using the Clausius-Mossotti equation from Ref. 35 with index of refraction data and density from Ref. 12.
- <sup>37</sup>Calculated using the Clausius-Mossotti equation from Ref. 35, the dielectric constant for liquid methane from Ref. 12, and density from K. R. Ramaprasad, J. Caldwell, and D. S. McClure, *Icarus* **35**, 400 (1978).
- <sup>38</sup>D. Vidal and M. Lallmand, *J. Chem. Phys.* **64**, 4293 (1976).
- <sup>39</sup>W. Tauchert, H. Jungblut, and W. F. Schmidt, *Can. J. Chem.* **55**, 1860 (1977).
- <sup>40</sup>J. J. P. Stewart, *J. Comp. Chem.* **10**, 209 (1989).
- <sup>41</sup>J. J. P. Stewart, *J. Comp. Chem.* **10**, 221 (1989).
- <sup>42</sup>HyperChem by Hypercube is a commercial software package which incorporates a friendly graphics interface with a variety of molecular modelling, semiempirical, and *ab initio* methods.
- <sup>43</sup>V. V. Vasilyev, *Acta Chim. Hungarica* **130**, 743 (1993); these calculations to  $n=16$  have been reproduced and extended it to  $n=136$ , M. D. Tissandier, A. D. Earhart, S. I. Muhammad, and J. V. Coe, in preparation; M. D. Tissandier, Ph.D. thesis, The Ohio State University (1997).
- <sup>44</sup>J. K. Gregory and D. C. Clary, *J. Phys. Chem.* **100**, 18 014 (1996).
- <sup>45</sup>K. Liu, J. D. Cruzan, and R. J. Saykally, *Science* **271**, 929 (1996).
- <sup>46</sup>S. S. Xantheas and T. H. Dunning, *J. Chem. Phys.* **99**, 8774 (1993).
- <sup>47</sup>S. S. Xantheas, *J. Chem. Phys.* **100**, 7523 (1994).
- <sup>48</sup>F. Huisken, M. Kaloudis, and A. Kulcke, *J. Chem. Phys.* **104**, 17 (1996).
- <sup>49</sup>J. K. Gregory, D. C. Clary, K. Liu, M. G. Brown, and R. J. Saykally, *Science* **275**, 814 (1997).
- <sup>50</sup>C. J. Tsai and K. D. Jordan, *Chem. Phys. Lett.* **213**, 181 (1993).
- <sup>51</sup>K. Liu, J. K. Gregory, M. G. Brown, C. Carter, R. J. Saykally, and D. C. Clary, *Nature* **381**, 501 (1996).
- <sup>52</sup>J. Kim, B. J. Mhin, S. J. Lee, and K. S. Kim, *Chem. Phys. Lett.* **219**, 243 (1994).
- <sup>53</sup>C. Gruenloh, J. Carney, C. Arrington, T. S. Zwier, S. Y. Fredericks and K. D. Jordan, *Science* (in press).
- <sup>54</sup>R. G. Mortimer, *Physical Chemistry* (Benjamin/Cummings, Redwood City, 1993), the drop radius in Eq. (5.5-18) can be related to the number of water molecules in the drop and used with the same relation for  $n+1$  to determine the free energy for adding a water molecule to the drop, see Fig. 5.18 for the physical context. Converting this relation to enthalpies gives  $\frac{8}{3}\pi N\partial(\gamma r_s^2/T)/\partial(1/T)$  for the constant, where  $\gamma$  is the surface tension,  $r_s$  is the effective radius of a water molecule, and  $N_0$  is Avagadro's number. A value of  $1.54\times 10^3$  dyne  $\text{cm}^{-1}$  bohr<sup>2</sup> for  $\partial(\gamma r_s^2/T)/\partial(1/T)$  determines the 0.226 eV value of the constant.
- <sup>55</sup>One could also use 0.443 eV for this constant to give a relation which roughly connects bulk to the calculated cluster values from I. P. Buffy and W. B. Brown, *Chem. Phys. Lett.* **109**, 59 (1984), avoiding the offset issue.
- <sup>56</sup>H. A. Schwarz and R. W. Dodson, *J. Phys. Chem.* **88**, 3643 (1984).
- <sup>57</sup>T. A. Milne, J. E. Beachey, and F. T. Greene, AFCRL Report 70-0341 (1970).
- <sup>58</sup>S. V. Olesik, Ph.D. thesis, University of Wisconsin-Madison (1982); photoionization of  $(\text{H}_2\text{O})_n$  clusters.
- <sup>59</sup>The lower end of our range of  $V_0$  values has been chosen as the preferred value in view of the relation between polarizability and  $V_0$  and the known optical polarizability of water, see the last paragraph of Sec. II A.
- <sup>60</sup>An enthalpic value of  $0.579\pm 0.012$  (95% conf.) is determined from experimental  $K_w$  vs  $T$  data in Ref. 12 by the slope of  $R \ln(K_w)$  vs  $1/T$ .
- <sup>61</sup>U. Sokolov and G. Stein, *J. Chem. Phys.* **44**, 3329 (1966).
- <sup>62</sup>J. W. Boyle, J. A. Ghormley, C. J. Hohanadel, and J. F. Riley, *J. Phys. Chem.* **73**, 2886 (1969).
- <sup>63</sup>The adiabatic energetic threshold determined in this work for seeing a hydrated electron from photoexcitation of water is 5.3 eV, so the observed threshold of 6.5 eV lies 1.2 eV above the minimum hydrated electron energy level, but 6.5 eV is not enough to access the conduction band, particularly when the associated reorganization energies are considered (see Fig. 5). The 10.06 eV PET of water suggests that 6.5 eV photons are about 3.6 eV shy of reaching the conduction band which is even too far to invoke electron-trapping states (however, lower values of the PET can change these arguments).
- <sup>64</sup>G. P. Parravicini and L. Resca, *Phys. Rev. B* **8**, 3009 (1973); Ref. 18 in this work explains that conduction bands were not calculated, but also how they might have been.
- <sup>65</sup>B. Baron and F. Williams, *J. Chem. Phys.* **64**, 3896 (1976).
- <sup>66</sup>B. Baron, D. Hoover, and F. Williams, *J. Chem. Phys.* **68**, 1997 (1978).
- <sup>67</sup>M. J. Campbell, J. Liesegang, J. D. Riley, R. C. G. Leckey, and J. G. Jenkin, *J. Electron Spectry. Relat. Phenom.* **15**, 83 (1979).
- <sup>68</sup>Figure 2 in the present work shows why the photoemission threshold of water does not determine the vacuum level as tentatively assumed in Fig. 3 of Ref. 8.
- <sup>69</sup>J. Hart and W. C. Gottschall, *J. Am. Chem. Soc.* **71**, 2102 (1967).
- <sup>70</sup>L. Kevan, *J. Phys. Chem.* **76**, 3830 (1972).
- <sup>71</sup>R. Onaka and T. Takahashi, *J. Phys. Soc. Jpn.* **24**, 548 (1968).
- <sup>72</sup>T. Shibaguchi, H. Onuki, and R. Onaka, *J. Phys. Soc. Jpn.* **42**, 152 (1977).